Inorg. Chem. **2008**, *47*, 7728−7733

Two- and Three-fold Interpenetrated Metal-Organic Frameworks from One-Pot Crystallization

Mohammad Hedayetullah Mir,[†] Susumu Kitagawa,[*,‡] and Jagadese J. Vittal[*,†]

Department of Chemistry, Faculty of Science, 3 Science Drive 3, National University of Singapore, Singapore 117543, and Department of Synthetic Chemistry and Biological Chemistry, Graduate School of Engineering, Kyoto University, Katsura, Kyoto 615-8510, Japan

Received April 28, 2008

Two different three-dimensional interpenetrating metal-organic frameworks, $\{[Co(bpe)(muco)](DMF)(H_2O)\}_n$ (**1**) and $\{[Co(bpe)(muco)(H_2O)_2]\cdot 4(H_2O)\}_n$ (**2**) [bpe = 4,4′-bipyridyl ethylene, H_2-muco = *trans,trans*-muconic acid, DMF = dimethyl formamide] have been co-crystallized in one-pot reaction. This work offers some insights into the intricacy of designing coordination polymers with variable interpenetration, showing new modes of entanglements. Single crystal X-ray diffraction analyses reveal that the compound **1** has a highly distorted cubic (α-Po) net with 2-fold interpenetrated structures while compound **2** displays a 3-fold interpenetrating net-work with an unprecedented 6^6 topology which is different from other well-known 4-connected nets such as diamond or hexagonal diamond. Despite varied interpenetrations, both compounds retain open channels, filled with aggregated guest solvent molecules. As far as the ratios of Co/muco/bpe are concerned, these two complexes can be considered as supramolecular isomers. Formation of a particular isomer in major quantity can be obtained by varying the countercation of the muconate salt in different solvents, by layering, and by changing the order of the components.

Introduction

In the past two decades, the design and synthesis of metal-organic frameworks (MOFs) by self-assembly of organic ligands as linkers and metal ions as connecting points have afforded a great deal of interest among the family of polymers, inorganic materials, and supramolecular architectures.[1,2] Of these, a large number of MOFs exhibiting large surface area and porosity retained upon the removal of the solvent molecules have attracted special interest due to their potential applications in gas storage, separation, ion-exchange, nonlinear optics, and catalysis.[3–6] The pore size and shape can be tuned by the judicious choice of metal-containing secondary building units and bridging organic linkers and by making the frameworks interpenetrating or interweaving.[7] By using various linkers differing in lengths of the of organic backbones, many MOFs with desired

* To whom correspondence should be addressed. E-mail: kitagawa@sbchem.kyoto-u.ac.jp (S.K.), chmjjv@nus.edu.sg (J.J.V.). Fax: +81-75-383-2732 (S.K.), +65-6779-1691 (J.J.V.).

† National University of Singapore.

‡ Kyoto University.

(1) (a) Bailar, J. C., Jr. *Perspective Inorganic Reaction*; Interscience: New York, 1964; Vol. *1*. (b) Desiraju, G. R. *Crystal Engineering, the Design of Organic Solids*; Elsevier: Amsterdam, 1989. (c) Janiak, C. *Angew. Chem., Int. Ed.* **1997**, *36*, 1431. (d) Batten, S. R.; Robson, R. *Angew.Chem., Int. Ed.* **1998**, *37*, 1460. (e) Eddaoudi, M.; Moler, D. B.; Li, H.; Chen, B.; Reineke, T. M.; O'Keeffe, M.; Yaghi, O. M. *Acc. Chem. Res.* **2001**, *34*, 319.

(2) (a) Zaworotko, M. J. *Chem. Soc. Rev.* **1994**, *23*, 283. (b) Moulton, B.; Zaworotko, M. J. *Chem. Rev.* **2001**, *101*, 1629. (c) Kitagawa, S.; Kitaura, R.; Noro, S.-I. *Angew.Chem., Int. Ed.* **2004**, *43*, 2334. (d) Lee, S.; Mallik, A. B.; Xu, Z.; Lobkovsky, E. B.; Tran, L. *Acc. Chem. Res.* **2005**, *38*, 251.

(3) (a) Yaghi, O. M.; Davis, C. E.; Li, G. M.; Li, H. *J. Am. Chem. Soc.* **1997**, *119*, 2861. (b) Zaworotko, M. J. *Angew. Chem., Int. Ed.* **2000**, *39*, 3052.

(4) (a) Seo, J. S.; Wang, D.; Lee, H.; Jun, S. I.; Oh, J.; Jeon, Y. J.; Kim, K. *Nature* **2000**, *404*, 982. (b) Eddaoudi, M.; Kim, J.; Rosi, N.; Vodak, D.; Wachter, J.; O'Keeffe, M.; Yaghi, O. M. *Science* **2002**, *295*, 469.

(5) (a) Rosi, N. L.; Eckert, J.; Eddaoudi, M.; Vodak, D. T.; Kim, J.; O'Keeffe, M.; Yaghi, O. M. *Science* **2003**, *300*, 1127. (b) Pan, L.; Sander, M. B.; Huang, X.; Li, J.; Smith, M.; Bittner, E.; Bockrath, B.; Johnson, J. K. *J. Am. Chem. Soc.* **2004**, *126*, 1308. (c) Dybtsev, D. N.; Chun, H.; Yoon, S. H.; Kim, D.; Kim, K. *J. Am. Chem. Soc.* **2004**, *126*, 32. (d) Kesanli, B.; Cui, Y.; Smith, M. R.; Bittner, E. W.; Bockrath, B. C.; Lin, W. *Angew.Chem., Int. Ed* **2005**, *44*, 72.

(6) (a) Suslick, K. S.; Bhyrappa, P.; Chou, J.-H.; Kosal, M. E.; Nakagaki, S.; Smithenry, D. W.; Wilson, S. R. *Acc. Chem. Res.* **2005**, *38*, 283. (b) Bradshaw, D.; Prior, T. J.; Cussen, E. J.; Claridge, J. B.; Rosseinsky, M. J. *J. Am. Chem. Soc.* **2004**, *126*, 6106. (c) Ohmori, O.; Fujita, M. *Chem.Commun.* **2004**, 1586. (d) Evans, O. R.; Ngo, H. L.; Lin, W. *J. Am. Chem. Soc.* **2001**, *123*, 10395.

(7) (a) Chen, B.; Eddaoudi, M.; Reineke, T. M.; Kampf, J. W.; O'Keeffe, M.; Yaghi, O. M. *J. Am. Chem. Soc.* **2000**, *122*, 11559. (b) Chen, B.; Eddaoudi, M.; Hyde, S. T.; O'Keeffe, M.; Yaghi, O. M. *Science* **2001**, *291*, 1021.

10.1021/ic800766q CCC: $40.75
Published on Web 07/29/2008

structures have been obtained[8] and the interpenetrated MOFs have been widely explored among them.[1d,9] The design and construction of the interpenetrated/entangled networks is an important focus in supramolecular chemistry for intriguing artistic and practical reasons. In this aspect, the longer dicarboxylates and bidentate pillar linkers have been extensively used in the formation of varied interpenetrated frameworks.[10,11] Therefore, the rigid spacer ligand with C_{2h} symmetry, *trans,trans*-muconic acid (H_2muco) as long dicarboxylate,[12–14] and 4,4′-bipyridine (4,4′-bpy) as bidentate pillar linkers have been introduced for the construction of the interpenetrated supramolecular architectures.

Of particular interest, the self-assembly of various kinds of coordination frameworks is one of the means to obtain coordination polymers with new modes of entanglements in the interpenetrating architectures. Herein, we report the self-assembly of H_2muco, a longer spacer ligand, 4,4′-bis(pyridyl)ethylene (bpe), and cobalt(II) ions by slow diffusion method. We obtained two three-dimensional (3D) interpenetrating structures with muconate anions, $\{[Co(bpe)(muco)](DMF)(H_2O)\}_n$ (**1**) and $\{[Co(bpe)(muco)(H_2O)_2]\cdot 4(H_2O)\}_n$ (**2**) formed in one-pot reaction. Concomitant crystallization of two polymorphs has been observed in the coordination compounds.[15] In this particular study, **1** and **2** are not polymorphs but can be classified as supramolecular isomers[2b,16] as far as the composition of Co/muco/bpe is concerned, which are responsible for the connectivity of the 3D structures. From the topological point of view; **1** has the commonly observed 6-connected distorted cubic (α-Po) type net[11,17] and **2** can be described in terms of 4-connected 6^6 which is attributed to all *cis*-geometry of the linkers. This topology appears to be different from commonly encountered 4-connected nets such as diamondoids and hexagonal diamondoids.

Experimental Section

All chemicals purchased were reagent grade and were used without further purification. The elemental analyses were carried out in the Microanalytical Laboratory, Department of Chemistry, National University of Singapore. The infrared (IR) spectra were recorded (400−4000 cm^{-1} region) on a FTS165 Bio-Rad FT-IR spectrometer using KBr pellets. Thermogravimetric analyses (TGA) were performed under a nitrogen atmosphere with a heating rate of 5 °C/min using an SDT 2960 TGA Thermal Analyzer. Variable temperature X-ray powder diffraction was performed using a Bruker-AXS D8 advance powder X-ray diffractometer with an Anton Paar Model HTK 1200 high temperature chamber.

Synthesis of Complexes 1 and 2. Stock solutions of $Co(NO_3)_2\cdot 6H_2O$ (0.291 g, 1 mmol) in 10 mL of H_2O, H_2muco (0.142 g, 1 mmol) neutralized with Et_3N (0.212 g, 2 mmol) in 10 mL of ethanol, and bpe (0.182 g, 1 mmol) in 10 mL of methanol were prepared. Then, 2 mL of bpe solution was carefully layered above the 2 mL of metal solution using 2 mL 1:1 (v/v) buffer solution of dimethylformamide (DMF) and MeOH followed by layering of 2 mL of muconate solution. The orange block shaped crystals of complex $\{[Co(bpe)(muco)](DMF)(H_2O)\}_n$ (**1**) were obtained after one week (0.066 g, yield 70%) along with some light

Table 1. Crystal Data and Refinement Parameters for Complexes **1** and **2**

Formula	$C_{21}H_{23}CoN_3O_6$ (**1**)	$C_{18}H_{24}CoN_2O_{10}$ (**2**)
fw	472.35	487.32
cryst syst	orthorhombic	monoclinic
space group	*Pbca*	*C2/c*
a (Å)	13.7170(6)	37.552(3)
b (Å)	14.7878(6)	13.1257(9)
c (Å)	21.0282(8)	9.4044(6)
α, deg	90	90
β, deg	90	103.218(2)
γ, deg	90	90
V, Å^3	4265.4(3)	4512.6(5)
Z	8	8
D_{calcd}, g cm^{-3}	1.471	1.435
μ, mm^{-1}	0.848	0.815
λ, Å	0.71073	0.71073
data [$I > 2\sigma(I)$]/params	2745/ 289	3563/ 315
GOF on F^2	1.027	1.030
final *R* indices [$I > 2\sigma(I)$][a,b]	R1 = 0.0595	R1 = 0.0434
	wR2 = 0.1533	wR2 = 0.1153
final *R* indices (all data)[a,b]	R1 = 0.0881	R1 = 0.0521
	wR2 = 0.1688	wR2 = 0.1221

[a] $R1 = \sum||F_o| - |F_c||/\sum|F_o|$. [b] $wR2 = [\sum w(F_o^2 - F_c^2)^2/\sum w(F_o^2)^2]^{1/2}$.

Table 2. Selected Bond Lengths and Bond Angles in **1** and **2**[a]

Complex **1**		Complex **2**	
Co(1)−O(3)	2.007(3)	Co(1)−O(3)	2.065(2)
Co(1)−O(4)a	2.026(3)	Co(1)−O(1)	2.090(2)
Co(1)−O(1)	2.134(3)	Co(1)−N(1)	2.113(2)
Co(1)−N(1)	2.152(4)	Co(1)−N(2)	2.144(2)
Co(1)−N(2)	2.159(4)	Co(1)−O(6)	2.151(2)
Co(1)−O(2)	2.283(4)	Co(1)−O(5)	2.161(2)
O(3)−Co(1)−O(4)a	122.95(14)	O(3)−Co(1)−O(1)	87.31(7)
O(3)−Co(1)−O(1)	148.78(14)	O(3)−Co(1)−N(1)	88.22(8)
O(4)a-Co(1)−O(1)	88.10(13)	O(1)−Co(1)−N(1)	89.34(8)
O(3)−Co(1)−N(1)	91.70(13)	O(3)−Co(1)−N(2)	91.88(8)
O(4)a-Co(1)−N(1)	90.56(13)	O(1)−Co(1)−N(2)	179.09(9)
O(1)−Co(1)−N(1)	91.06(13)	N(1)−Co(1)−N(2)	91.06(9)
O(3)−Co(1)−N(2)	87.74(13)	O(3)−Co(1)−O(6)	175.31(7)
O(4)a-Co(1)−N(2)	87.45(13)	O(1)−Co(1)−O(6)	88.40(7)
O(1)−Co(1)−N(2)	90.85(13)	N(1)−Co(1)−O(6)	89.83(8)
N(1)−Co(1)−N(2)	177.20(14)	N(2)−Co(1)−O(6)	92.42(8)
O(3)−Co(1)−O(2)	89.84(13)	O(3)−Co(1)−O(5)	92.89(7)
O(4)a-Co(1)−O(2)	147.19(12)	O(1)−Co(1)−O(5)	90.68(7)
O(1)−Co(1)−O(2)	59.11(12)	N(1)−Co(1)−O(5)	178.89(8)
N(1)−Co(1)−O(2)	89.12(13)	N(2)−Co(1)−O(5)	88.94(8)
N(2)−Co(1)−O(2)	93.63(13)	O(6)−Co(1)−O(5)	89.06(7)

[a] Symmetry transformations used to generate equivalent atoms: a: $-x + 1, -y, -z + 1$.

(8) (a) Kitaura, R.; Fujimoto, K.; Noro, S. I.; Kondo, M.; Kitagawa, S. *Angew.Chem., Int. Ed.* **2002**, *41*, 133. (b) Kitaura, R.; Seki, K.; Akiyama, G.; Kitagawa, S. *Angew.Chem., Int. Ed.* **2003**, *42*, 4. (c) Kitagawa, S.; Uemura, K. *Chem. Soc. Rev.* **2005**, *34*, 109. (d) Rowsell, J. L. C.; Yaghi, O. M. *Nanoporous Mesoporous Mater.* **2004**, *73*, 4.

(9) See the web site set up by Dr. S. R. Batten: http://www.chem.monash.edu.au/staff/sbatten/interpen/ (accessed February 2008).

(10) Carlucci, L.; Ciani, G.; Proserpio, D. M. *Coord. Chem. Rev.* **2003**, *246*, 247.

(11) (a) Chen, B.; Ma, S.; Hurtado, E. J.; Lobkovsky, E. B.; Zhou, H. C. *Inorg. Chem.* **2007**, *46*, 8490. (b) Li, X. H.; Yang, S. Z.; Xiao, H. P. *Cryst. Growth Des.* **2006**, *6*, 2392.

(12) Cotton, F. A.; Donahue, J. P.; Murillo, C. A. *J. Am. Chem. Soc.* **2003**, *125*, 5436.

(13) Mukherjee, P. S.; Das, N.; Kryschenko, Y. K.; Arif, A. M.; Stang, P. J. *J. Am. Chem. Soc.* **2004**, *126*, 2464.

(14) Burrows, A. D.; Mingos, D. M. P.; Lawrence, S. E.; White, A. J. P.; Williams, D. J. *J. Chem. Soc., Dalton Trans.* **1997**, 1295.

(15) (a) Bernstein, J.; Davey, R. J.; Henck, J. O. *Angew.Chem., Int. Ed.* **1999**, *38*, 3440. (b) Holmes, K. E.; Kelly, P. F.; Elsegood, M. R. J. *CrystEngComm* **2002**, *4*, 545. (c) Fromm, K. M.; Doimeadios, J. L. S.; Robin, A. Y. *Chem. Commun.* **2005**, 4548. (d) Braga, D.; Cojazzi, G.; Emiliani, D.; Maini, L.; Polito, M.; Gobetto, R.; Grepioni, F. *CrystEngComm* **2002**, *4*, 277. (e) Hamamci, S.; Yilmaz, V. T.; Buyukgungor, O. *Acta Crystallogr., Sect. C* **2006**, *62*, M1.

(16) (a) Abourahma, H.; Moulton, B.; Kravtsov, V.; Zaworotko, M. J. *J. Am. Chem. Soc.* **2002**, *124*, 9990. (b) Mahmoudkhani, A. H.; Shimizu, G. K. H. *Inorg. Chem.* **2007**, *46*, 1593.

orange platy crystals of $\{[Co(bpe)(muco)(H_2O)_2]\cdot 4(H_2O)\}_n$ (**2**) (0.010 g, yield 10%). The crystals were separated by hand picking, washed with a MeOH and H_2O (1:1) mixture, and dried. Elemental analysis calcd. for $C_{21}H_{23}CoN_3O_6$ (**1**): C, 53.40; H, 4.91; N, 8.90, Found: C, 53.22; H, 4.80; N, 8.86. IR (KBr pellet, cm^{-1}): 1618 $\nu_{as}(COO^-)$, 1423 $\nu_{sys}(COO^-)$. Thermogravimetry (TG) weight loss of 18.6% observed for the fresh sample **1** matched with 19.3% for the loss of one DMF and one H_2O molecule.

Complex **2** was prepared as major product by the following method. Stock solutions of $Co(NO_3)_2\cdot 6H_2O$ (0.291 g, 1 mmol) in 10 mL of ethanol, H_2muco (0.142 g, 1 mmol) neutralized with NaOH (0.080, 2 mmol) in 10 mL of H_2O, and bpe (0.182 g, 1 mmol) in 10 mL of methanol were prepared. Then, 2 mL of the bpe solution was layered over 2 mL of aqueous Na_2-muco solution using the 2 mL buffer solution of 1:1 (v/v) DMF and MeOH followed by the layering of 2 mL of metal solution. The light orange platy shaped crystals of **2** were obtained after a few days (0.058 g, yield 60%) along with some dark orange block crystals of **1** (0.009 g, yield 10%). The crystals were separated by hand picking and washed with MeOH and H_2O (1:1). Elemental analysis calcd. for $C_{18}H_{26}CoN_2O_{10}$ (**2**): C, 44.18; H, 5.36; N, 5.72, Found: C, 44.25; H, 4.98; N, 5.80. IR (KBr pellet, cm^{-1}): 3447 ν (O−H), 3423 ν (O−H), 1615 ν (COO^-), 1421 $\nu_{sys}(COO^-)$. TG weight loss for the fresh sample **2** calcd for 6 H_2O: 21.3%; found: 22.0%.

General X-ray Crystallography. Single Crystals suitable for data collection obtained during synthesis were chosen under an optical microscope, mounted on glass fibers, and frozen under a stream of cryogenic nitrogen gas before data collection. Crystal data were collected on a Bruker APEX diffractometer attached with a charge-coupled device (CCD) detector and graphite-monochromated Mo Kα radiation (λ, 0.71073 Å) at 223 K. An empirical absorption correction was applied to the data using the *SADABS* program.[18] Both the structures were solved by direct methods using and refined on F^2 by full-matrix least-squares procedures with SHELXTL.[19] The crystallographic data for **1** and **2** are summarized in Table 1, and selected bond lengths and bond angles are given in Table 2. All non-hydrogen atoms were refined with anisotropic displacement parameters except for the disordered atoms. The C−H hydrogen atoms are added in calculated positions and the positional and common isotropic thermal parameters of hydrogen atoms in water molecules. In **2**, three of the four lattice water molecules were disordered over 10 positions with occupancies varying from 0.125 to 0.5. However, positional and common isotropic thermal parameters of hydrogen atoms of aqua ligands were refined in the least-squares cycles.

Results and Discussion

The two solid-state compounds **1** and **2** were obtained in a one-pot crystallization. On the other hand, these compounds were also obtained as major products by changing the reaction conditions. Compound **1** was obtained as the major project from three layer diffusion containing triethylamine salt of *trans*-muconic acid (top), bpe (middle), and cobalt nitrate solution (bottom). On the other hand, when cobalt nitrate solution was used as top layer and sodium salt of *trans*-muconic acid as bottom layer with bpe in the middle layer, **2** was formed as the major product. X-ray powder diffraction patterns were recorded for the unseparated bulk of the samples obtained in the synthesis as well as pure **1** and **2** crystals. The patterns for the bulk matched well with those from **1** and **2** indicating that only two types of products were obtained (Supporting Information). The X-ray powder patterns of **1** and **2** were also matched with the simulated patterns generated from the single crystals data. Although **1** and **2** differ much in terms of structural motifs, they are solvent-included crystalline solids and have same Co/bpe/muco ratio in the 3D structures. Both form neutral interpenetrated MOFs with small open channels filled with guest solvent molecules. The crystals were distinctly different in terms of color and morphology. Compound **1** formed as deep orange blocks, whereas **2** formed as light orange platy crystals. In the solid state, **1** has a 2-fold interpenetrated cubic net, and calculations using PLATON[20] show that the effective volume occupied by solvents is 1225.0 $Å^3$ per unit cell, which is 28.7% of the cell volume. Compound **2** has a 3-fold interpenetrated (4,4)-connected net with the volume of 1075.6 $Å^3$ per unit cell (23.8% of the unit cell volume) occupied by the lattice water molecules.

Structure of 1. In **1**, $\{[Co(bpe)(muco)](DMF)(H_2O)\}_n$, each Co(II) center has a pair of bpe ligands disposed in *trans*-fashion and a chelating muco ligand. Of these, two muco anions act as bridging ligands between two Co(II) atoms and align a pair of bpe ligands to form a ladder polymer (Co−O = 2.007(3)−2.283(4) Å and Co−N = 2.152(4)−2.159(4) Å) (Figure 1). The coordination geometry at Co(II) is a distorted octahedron, and the bpe ligands are propagating along the *a*-axis. The Co···Co distance in the ladder is 4.026 Å. The pyridyl rings are aligned in parallel with a $\pi\cdots\pi$ distance of 3.868 Å. The Co−bpe−Co distance is equal to the *a*-axis in the cell, 13.717 Å. The butadiene group of the muco ligand interconnects the "$Co_2(muco)_{4/2}$" building blocks to form a (4,4) net in *bc* plane. If the centers of the Co_2 dimers are connected in this plane, it forms a rhombus with the side length of 12.854 Å. The diagonal distances of the rhombus are equal to the lengths of the *b* and *c* axes of the unit cell, 14.788 and 21.028 Å, respectively. Binuclear subunits constitute the nodes of the net structure, and the connectivity of their centroids lead to a highly distorted cubic (α-Po) type structure.[11,17] The large cavity space is reduced by two- fold interpenetration (Figure 2). Small cavities left behind are filled by DMF-H_2O solvents which are strongly interacting through C═O···H−O−H bonds (O···H = 1.92 Å, O···O = 2.831 Å, ∠O···O−H = 167°). Again, the guest water molecule is strongly hydrogen bonded to the oxygen atom of chelating muco ligand (O···H = 1.87 Å, O···O = 2.788 Å, ∠O···O−H = 167°) (Supporting Information).

(17) (a) Hoskins, B. F.; Robson, R.; Scarlett, N. V. Y. *J.Chem. Soc., Chem. Commun.* **1994**, 2025. (b) Duncan, P. C. M.; Goodgame, D. M. L.; Menzer, S.; Williams, D. J. *Chem.Commun.* **1996**, 2127. (c) Desmartin, P. G.; Williams, A. F.; Bernardinelli, G. *New.J. Chem.* **1995**, *19*, 1109. (d) Dong, W.; Zhu, L.-N.; Sun, Y.-Q.; Liang, M.; Liu, Z.-Q.; Liao, D.-Z.; Jiang, Z.-H.; Yan, S.-P.; Cheng, P. *Chem.Commun.* **2003**, 2544. (e) Matthews, C. J.; Elsegood, M. R. J.; Bernardinelli, G.; Clegg, W.; Williams, A. F. *Dalton Trans.* **2004**, 497.

(18) Sheldrick, G. M. *SADABS, Program for Empirical Absorption Correction for Area Detector Data*; University of Göttingen: Göttingen, Germany, 2000.

(19) *SHELXTL Reference Manual*, Version 5.1; Bruker AXS, Inc.: Madison, WI, 1997.

(20) Spek, A. L. *PLATON. A Multipurpose Crystallographic Tool*; Utrecht University: Utrecht, The Netherlands, 2003.

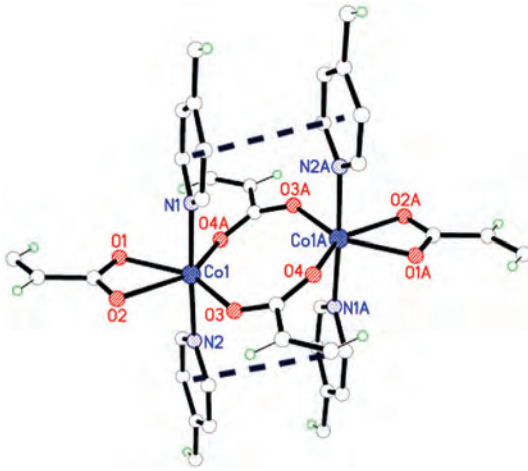

Figure 1. Perspective view showing the orientation of bpe and muco ligands in the dimeric repeating unit of **1**. Dashed lines show $\pi\cdots\pi$ interactions between bpe molecules. The solvent molecules and the hydrogen atoms in pyridyl rings are not shown for the clarity.

Structure of 2. In **2** $\{[Co(bpe)(muco)(H_2O)_2](H_2O)_3\}_n$, each Co(II) is coordinated to two bpe (Co−N = 2.10(1)−2.14(1) Å), two monodentate muco ligands (Co−O = 2.067(8)−2.080(8) Å), and two water molecules (Co−O = 2.152(8) Å) all in *cis*- fashion. The topology is subsequently controlled by the connectivity of these spacer ligands to the metal ions. In the *ab* plane six Co(II) form a distorted-rectangular ring. Each shorter side is connected by a muco ligand and the longer side by a bpe and muco ligands. In other words, four muco, two bpe ligands, and six Co(II) form the distorted-rectangular ring. The Co−muco−Co and Co−bpe−Co distances are 11.037 Å and 13.687 Å, respectively. The extended structure in the *ab* plane is therefore formed as a brick-layered 2D net mainly attributed to *cis*-geometry muco ligands at the Co(II) centers (Figure 3). The alternate Co(II) centers of these rectangles are connected by bpe ligands up and down directions approximately along the *c*-axis perpendicular to the rectangles forming the 3D network structure. The length and width of the rectangle based on Co···Co distances are 24.676 Å and 11.037 Å, respectively. The distortion of the rectangle is evident from the Co−Co−Co angles, 110.64° and 72.97°. The large empty spaces provided by these rectangles are filled by 3-fold interpenetration of the 3D framework structures as shown in Figure 4.

Each distorted-rectangular ring has six Co(II) centers leading to the formation of a hexagon which is the shortest circuit here. For *p*-connected nodes, there are $p(p-1)/2$ unique pairs of links around a node, and the number of the shortest circuits for each unique pair of links is six. Hence, the Schläfli symbol is 6^6. Viewed from the *a*-axis, the puckered hexagonal layers in the *bc* plane are interconnected to give a net which is different from other well-known 4-connected nets such as diamondoid or hexagonal daimondoid which are also 6^6 as noted by Wells.[21] The known 3D uninodal 4-connected nets of MOFs are dominated by the tetrahedral geometry along with comparatively small contributions of square geometry or square and tetrahedral mixed geometry.[22] Thus, the topology of network of **2** is unusual because of the unique *cis*-geometry of the $[Co(bpe)_2(muco)_2(H_2O)_2]$ nodes.

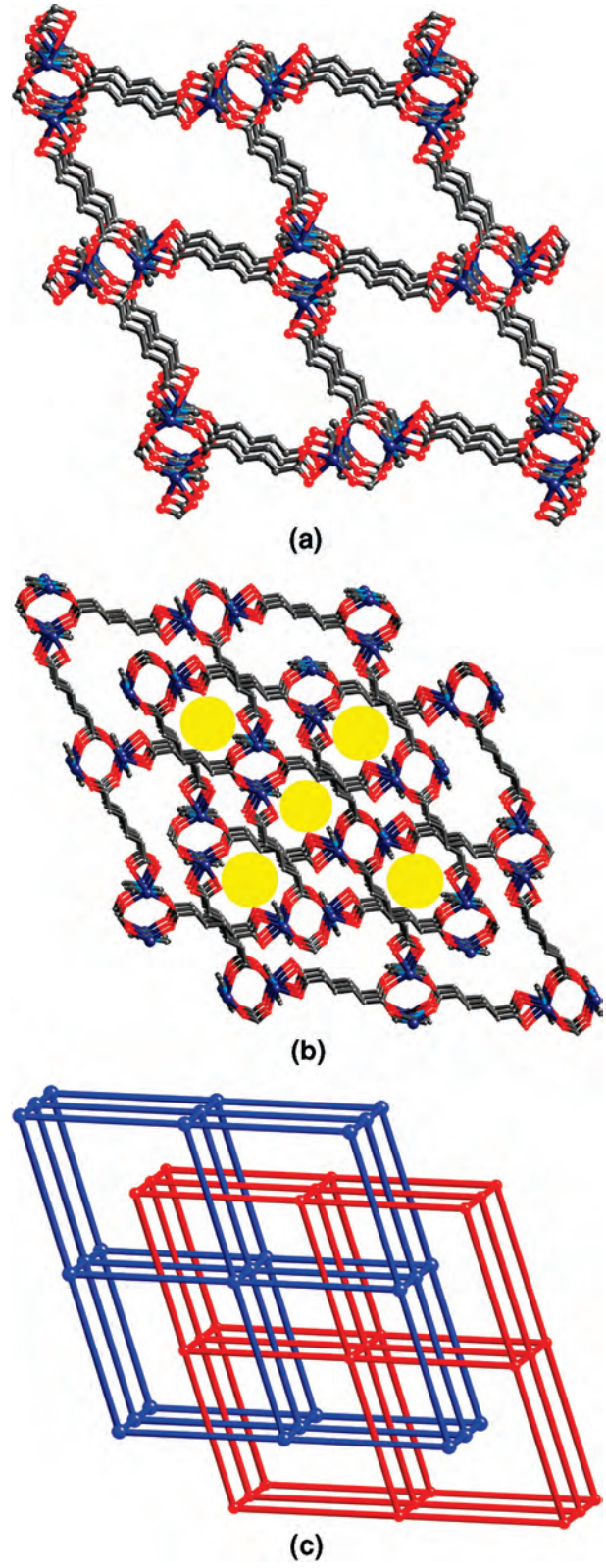

Figure 2. (a) One of the two independent distorted cubic nets of **1**. (b) Interpenetrated network of **1** viewed along the *a*-axis showing the presence of channels shown by yellow circles. Hydrogen atoms and guest molecules have been omitted. (c) Schematic diagram of the 2-fold interpenetrated cubic net of **1** joining the centers of the binuclear Co_2 subunits.

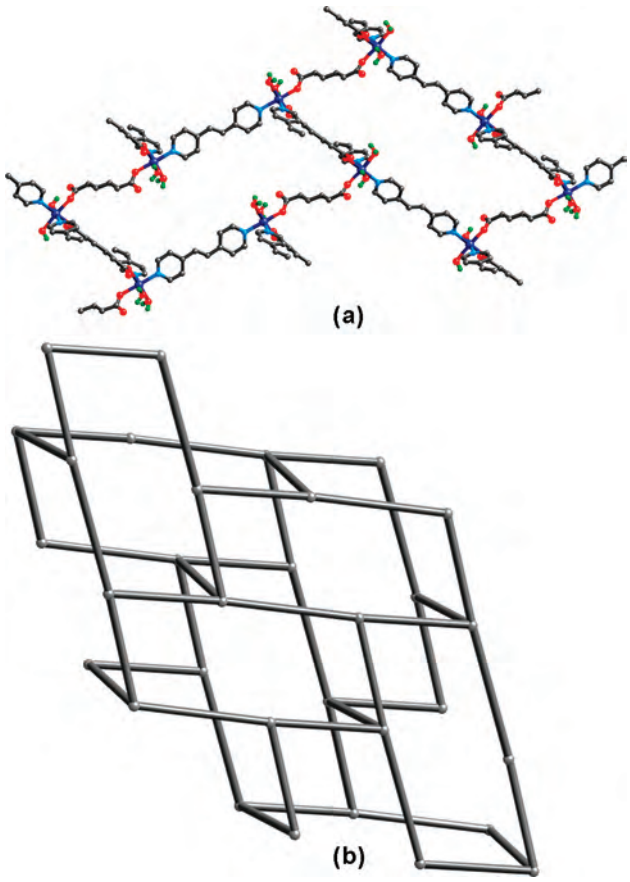

Figure 3. Connectivity showing the formation of hexagons by linking *cis*-$[Co(bpe)_2(muco)_2(H_2O)_2]$ nodes (a), and a schematic diagram showing a 4-connected uninodal net observed in **2** (b). Pyridyl groups of bpe and carboxylate units of muco ligands are shown as rods.

Even after 3-fold interpenetration, **2** still possesses some void space where disordered water molecules have been located along the *c*-axis shown in Figure 4b. Guest water molecules interact with the coordinated water molecules through hydrogen bonding (O6−H6B···O7 and O8−HA···O5). Additional hydrogen bonds are formed between coordinated water molecules and carboxylate oxygen atoms. The coordinated water molecules act as terminal ligands, and they are intra- and intermolecularly hydrogen bonded to carboxylate oxygen atoms of muco ligands (O5−H5A···O2, O5−H5B···O4 and O8−H8A···O5) (Supporting Information).

Thermal Stability of Compound 1 and 2. The thermal stability of compound **1** has been studied by TG and variable temperature powder X-ray diffraction (XRD). The TG shows the loss of DMF and water occurs in the temperature region 70−180 °C (weight loss found, 18.6%, and calculated, 19.3%). The powder XRD of the sample heated to 200 °C under vacuum and cooled to room temperature in air (Supporting Information) matched with that of the bulk showing that the crystal structure is retained after the solvent removal. While the powder XRD recorded at 200 °C shows additions peaks and intensity variation indicating the possibility of a phase transition at this temperature. After the removal of solvents, the single crystals maintain the morphology but they do not diffract strongly for data collection.

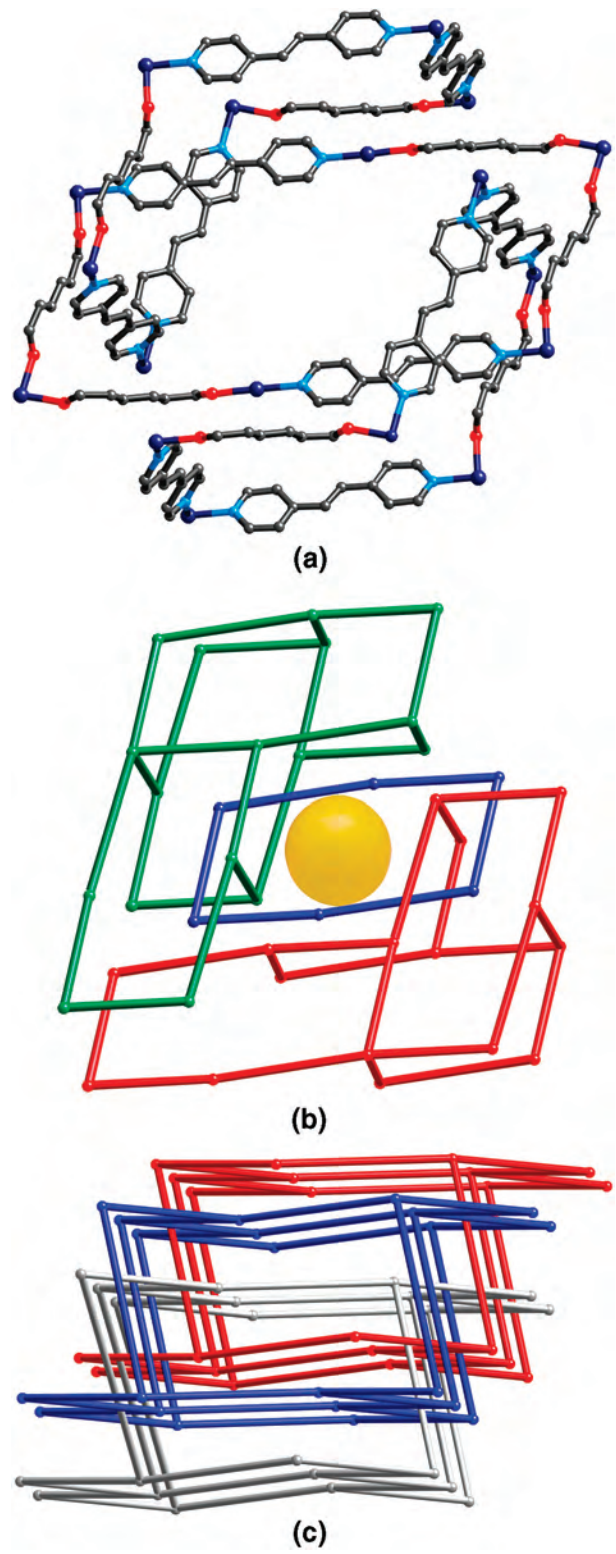

Figure 4. (a) Details of 3-fold interpenetration in **2**. (b) Schematic diagram showing the details of interpenetration around a single rectangle and region occupied by water molecules by yellow sphere. (c) Schematic representation of the 3-fold interpenetration obtained by connecting the metal centers in **2**.

(21) (a) Wells, A. F. *Three-Dimensional Nets and Polyhedra*; John Wiley & Sons: New York, 1977. (b) Wells, A. F. *Further Studies of Three-dimensional Nets*; ACA Monograph No. 8; American Crystallographic Association: Buffalo, NY, 1979. (c) Sasa, M.; Tanaka, K.; Bu, X. H.; Shiro, M.; Shionoya, M. *J. Am. Chem. Soc.* **2001**, *123*, 10750.
(22) Ockwig, N. W.; Delgado-Friedrichs, O.; O'Keeffe, M.; Yaghi, O. M. *Acc. Chem. Res.* **2005**, *38*, 176.

When **1** was evacuated under vacuum at 160 °C and the dehydrated sample was then exposed to water vapor, it takes back about three water molecules as determined by TG. Preliminary experiments indicated that **1** does not have a nitrogen gas sorption property at low temperatures. TG of compound **2** shows the loss of water molecules at 30−180 °C. The weight loss occurred in two stages corresponding to loss of lattice water and coordinated water molecules. The total loss of 21.3% corresponds to loss of all water molecules (calcd: 22.0%). The complete decomposition of the compound occurs above 300 °C.

This particular study represents the delicacy in designing interpenetrated frameworks with nanoporous open channels resulting from single crystallization. The composition of **1** and **2** differ only by solvent molecules, so they can be described as pseudo supramolecular isomers. The solid state structure of **1** is made up of novel distorted cuboidal building blocks, and the aggregation of the building blocks results in three-dimensional networks displaying 2-fold interpenetration. Despite the incidence of interpenetration, **1** still retains a nanoporous channel along the *c*-axis filled with a strong aggregation of H_2O-DMF molecules. Interestingly, these guest molecules can be removed from **1** at high temperature without it losing its crystallinity. Compound **2** is particularly interesting as it shows the unusual topology in its three-dimensional net (Figure 4c). Despite a higher degree of interpenetration, it retains a nanoporous open channel. Several intramolecular hydrogen bonds provide an additional stabilization within the $[Co(bpe)_2(muco)_2(H_2O)_2]$ unit. Although the compositions of the metal−ligands ratios are same for both compounds, the coordination modes of the ligands are distinctly different. The muco ligands coordinate to Co(II) in monodentate manner in **2** which allows two water molecules to bind to the metal ions. The all *cis*-geometry in **2** is responsible for a different topological structure in **2**.

Conclusions

We have reported two solvent accessible coordination compounds formed in a one-pot crystallization. Compound **1** is a 3D 2-fold interpenetrated distorted cubic net structure which includes water and DMF guest molecules. Compound **2** is an interesting 3D 3-fold interpenetrated MOF with an unusual 4-connected network topology as a result of the *cis*-configuration of the $[Co(bpe)_2(muco)_2(H_2O)_2]$ nodes. As the composition of the components involved in the construction of the 3D frameworks are the same for both compounds, they can be considered as supramolecular isomers.

Acknowledgment. The authors thank the Ministry of Education, Singapore for financial support of this research through the National University of Singapore Grant R-143-000-283-112 and Ms. Geok Kheng Tan and Prof. Koh Lip Lin for collecting X-ray data. We thank the referees for helpful suggestions.

Supporting Information Available: X-ray crystallographic files for compound **1** and **2** in a CIF file and powder XRD patterns, TGA plots, tables of selected bond lengths and bond angles, and some additional figures in a PDF file. This material is available free of charge via the Internet at http://pubs.acs.org.

IC800766Q